

CSC Electronics Performance Study at the beam.

Brookhaven National Laboratory

22 May 2000

Abstract

The prototype of front-end electronics (amplifier and Switch Capacitance Array (SCA)) was tested with the CSC chamber on the beam at the X5 high radiation facility at CERN. The beam test demonstrated that the new electronics worked reliably at maximum background rate. The analysis of the beamtest data was dedicated the impact of the sampling readout on the CSC performance. The several amplitude finding algorithms was checked. The dependence the CSC resolution and efficiency on ADC precision was studied also. The comparison the previous analysis has showed that at the same condition the results are similar for both beamtest.

1 Experimental set-up

During the October of 1999 the CSC prototype was tested at the X5 high radiation facility at CERN. The aim of this test was to get the first view at the prototypes of the front-end electronics (amplifiers and SCA).The CSC prototype and the Si telescope were the same as the previous beamtest-98. Fig.1 shows the layout of the beam test set-up. The Silicon microstrip telescope (Si) was installed at 1.5m from the CSC prototype and used to determine track parameters at the CSC position. The track position predicted by the Si telescope was used to measure CSC position resolution and track efficiency. Muon beam momentum was 80 Gev/c. Beam divergence at this momentum was 1.7 mrad. This enables to estimate the CSC resolution by comparison of the track

positions in two CSC layers with the precision good enough for quick on-line monitoring. The beam illuminated area of the chambers was determined by the $5 \times 5 \text{ cm}^2$ trigger counters (Sc1, Sc2). The high intensity radioactive gamma source ^{137}Cs was installed in the beam area. The variable lead absorbers were used to change the radiation flux intensity. The CSC prototype was placed at the distance of 1.5 m. from the gamma source. At this distance the open source provides the radiation background close to the one expected in the ATLAS at CSC position with the conventional safety factor 5 was taken into account.

The chamber parameters are following: anode-cathode spacing - 2.5 mm, anode wire diameter - $30 \mu\text{m}$, the wire pitch - 2.5 mm, 20 anode wires join to one anode group, cathode strip readout pitch - 5 mm, this distance contains three equal strips, one of them is the readout and the other two are intermediate strips. In this test the gas composition was $0.6\text{Ar} + 0.3\text{CO}_2 + 0.1\text{C}_2\text{H}_2\text{F}_4$. The gas gain was about 10^5 .

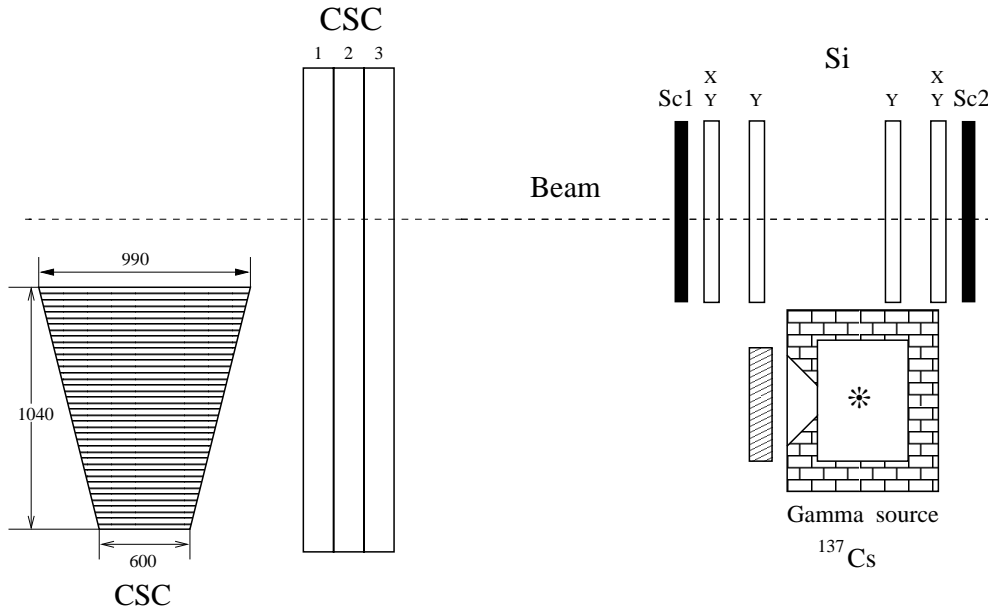


Figure 1: Beam test set-up layout.

Two kinds of amplifiers were used during this test. One CSC layer was equipped by prototype of the new amplifier chip, developed by BNL. The second plane was equipped by hybrid preamplifier and shaping amplifier of the old type. Signals from amplifiers were sampled, digitised and read out by the Switch Capacitance Array (SCA). The SCA has a 14 bit ADC, 40 MHz write clock and

pine-line of 144 cells. Each trigger selected event was registered in 16 time samples with average signal maximum placed in ninth sample. The trigger was not synchronised with the SCA write clock, thus there was an additional 25 nsec uncertainty in the time position of the signal relative to the time samples. The own SCA noise was about five ADC counts. The shape of the amplifier signal was bipolar and the width of the positive part of the signal was 80 nsec (fwhm) for new amplifier and 120 nsec for the old one (fig.2). The curves on the fig.2 is the fit by the bipolar function:

$$f(z) = A \cdot \left(1 - \frac{z}{n+1}\right) \cdot z^n \cdot e^{-z}, \quad (1.1)$$

where n is a number of amplifier integration ($n = 12$ for new amplifier and $n = 6$ for old amplifier), $z = (t - t_0)/\tau$, τ is parameter reflected the width of the signal ($fwhm = 1.5 \cdot \tau \cdot \sqrt{n-1}$), t_0 is the start position of the signal.

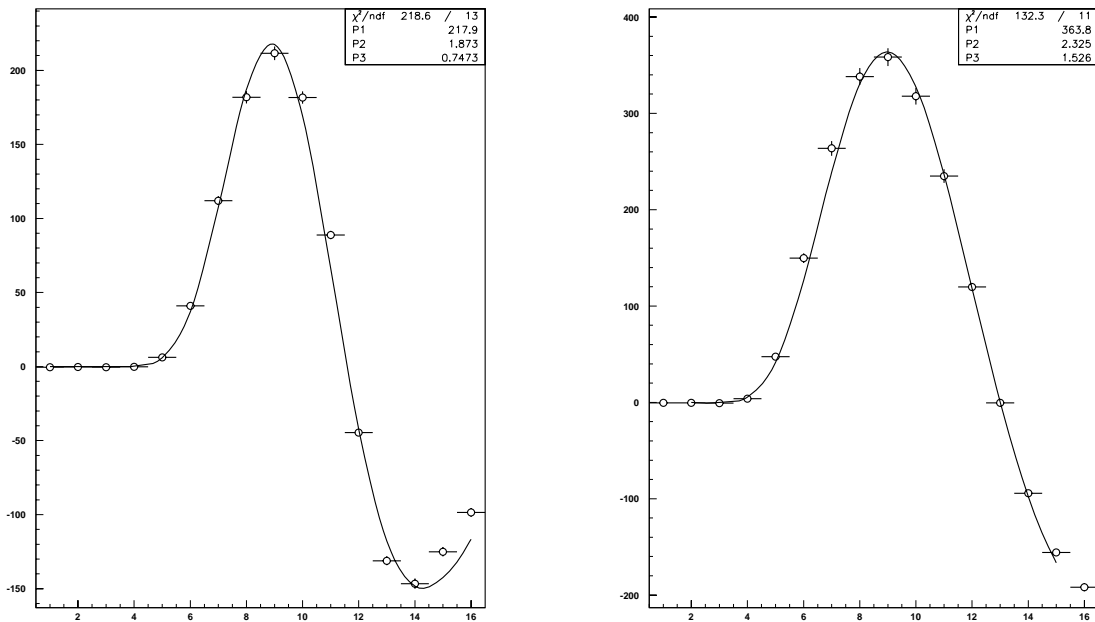


Figure 2: Measured average shape of signal from a) the new amplifier b) the old amplifier. The curves are the bipolar function fit.

The equivalent noise charge for both amplifiers was 3500 e. Perhaps, there was some contribution

to the noise from the environment. To unify the electronics gain of all channels the calibration was carried on regularly on a daily basis. For this purpose the amplitudes of the precision pulser were provided to one of the anode group and through the anode-cathode capacitances were provided for each cathode strips. This calibration was able to achieve the uniformity of the neighbouring channels better than 0.5 percent. For each strip the average amplitude of the second sample from the same run was used as pedestal.

2 Data analysis and results

The detail study of the CSC performance at low rates has been done in our previous works [1,2]. The factors affected the high rate CSC performance was considered in the Atlas note [3]. Here we will consider new factors which arise from the registration shape of signal due to time sampling.

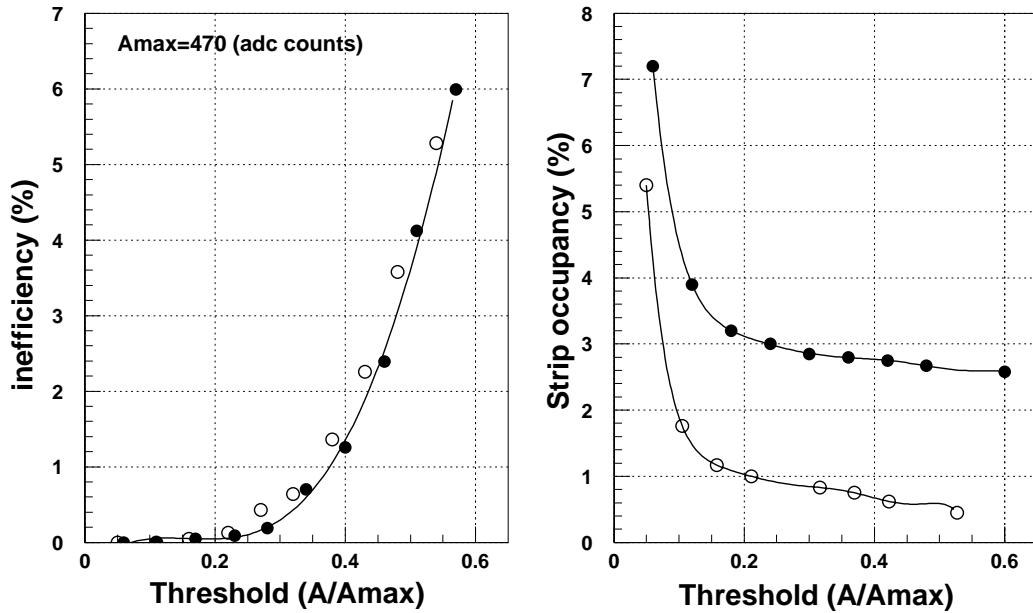


Figure 3: a) Cluster finding inefficiency versus threshold value. The threshold is normalised to Amax - most probable value of amplitude distribution in maximal strip. b) Probability of the fake hits per one strip versus threshold value.

The procedure of selection events for analysis was following. First of all, to select the perfect muon tracks some cuts were included: 1. all six Si planes should contain hits, 2. the track angle should be less $\pm 2mrad$, 3. when the efficiency of one of the CSC layer was studied another layer must contained hit near the track ($\pm 0.3mm$). The next step was to find clusters in the chamber. The event information from one layer is divided by strips and samples into 12x16 bins (12 strips and 16 t-samples). If the bin with a maximal amplitude was higher than the threshold, the event was selected for further analysis.

On the fig.3a a cluster inefficiency is shown versus the value of the threshold. For convenience, the threshold is normalised to the most probable amplitude of the charge deposited by the muon in the maximal strip. The fig.3b shows the probability per one strip to find a fake cluster at maximal available in this beamtest background rate $1.9 kHz/cm^2$ (the maximal expected LHC background rate at rapidity 2.7 is $2.6 kHz/cm^2$, if the factor safety five is taking into account).

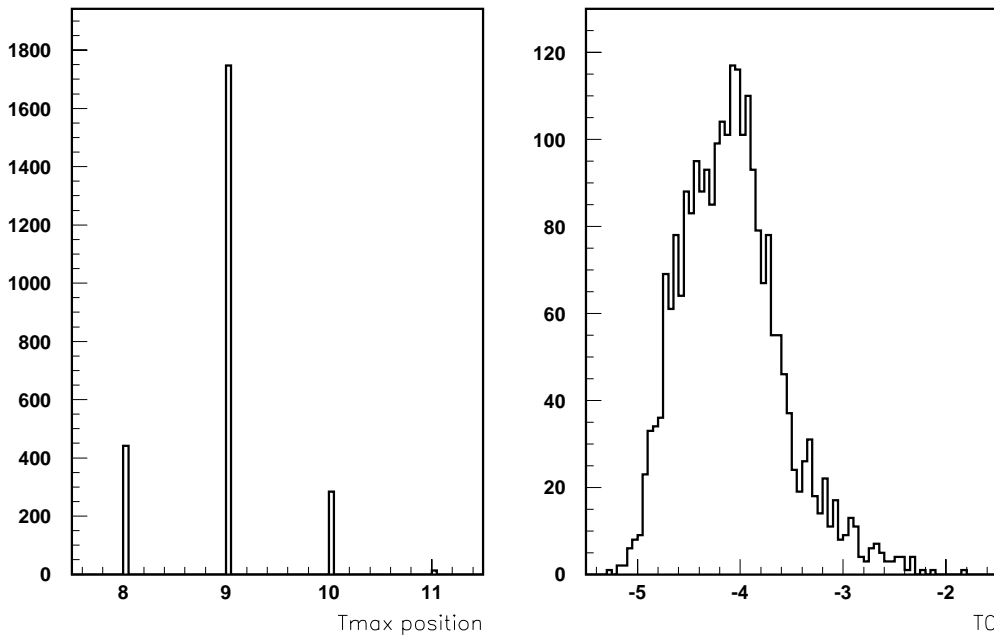


Figure 4: a) The maximal sample position. X axis in numbers of time sample. b) The time distribution of T_0 (signal beginning time).

The one strip probability may be used to evaluate the number of fake clusters per one trigger and per one plane at the maximum expected LHC background rate. It can be seen from fig.3a,b that optimal threshold is .25, the probability to find a fake cluster at this threshold is 3%, the rapidity of the strip k can be calculated from the formula $\eta_k = -\ln((r_0 + 0.5 \cdot k)/2L)$ (L is Z position first muon station, r_0 is radial position of lowest strip), the dependence of the background rate per strip on rapidity is published in our Atlas note [3], so, joining all together, the total number of fake clusters in one plane per one trigger is equal 4.2.

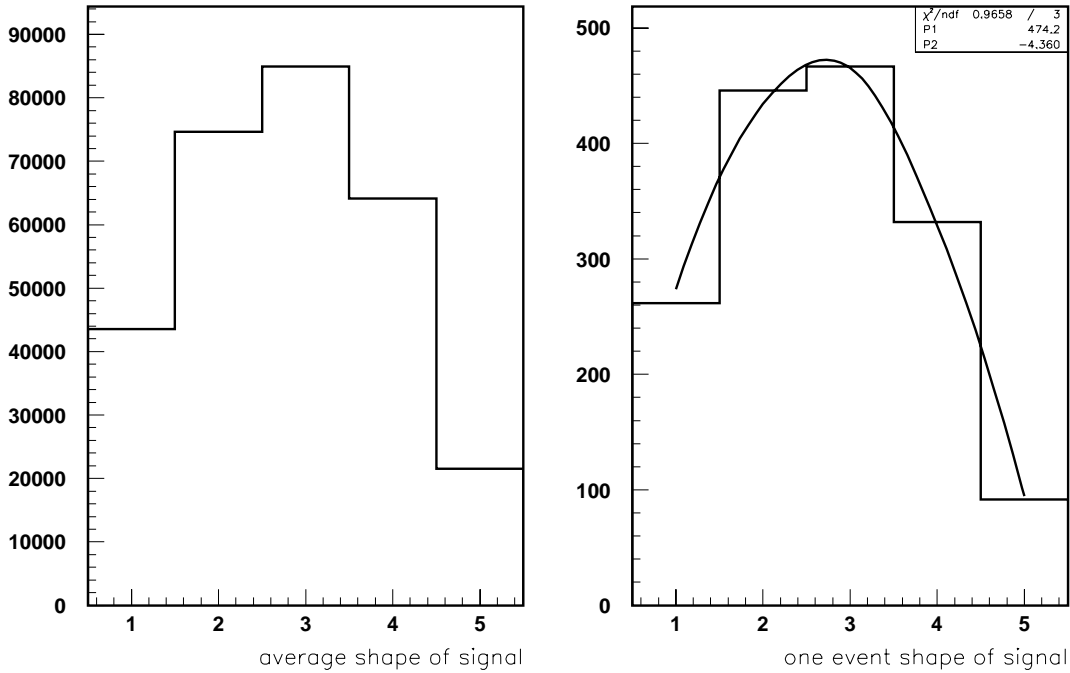


Figure 5: a) The average signal. b) The individual signal. The curve is the fit by bipolar function.

The amplitude finding algorithm is important to get a good position resolution. Indeed, even one percent amplitude uncertainty leads to an additional 50 micron contribution to the CSC position resolution. In previous tests we have used for the digitization a standard QDC or a pick sensitive ADC, in both cases the amplitude of the signal was defined by a hardware. In the case of SCA the signal time profile is registered instead, and the amplitude of the signal maximum should be defined by some algorithm. Potentially, this procedure may increase the error because the time position of

signal fluctuates due to the electron drift time and lack of synchronisation of the SCA write clock and the muon trigger. The fig.4 shows the distributions of the arrival time of the maximal sample (fig.4a) and the time of beginning of signal T0 (fig.4b). The value of T0 was found from the fit of signal by bipolar function. It can be seen that the fluctuations of the signal position are significant. The probability to find the position of maximal sample farther than one sample from the average position is 0.6%

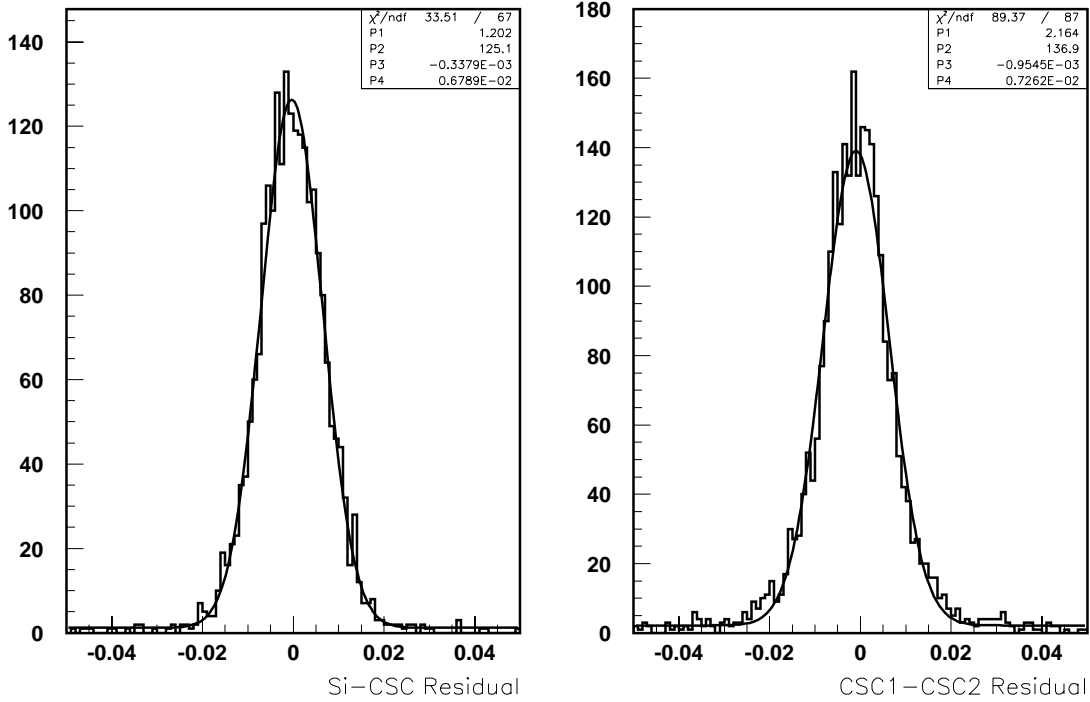


Figure 6: a) The Si-CSC1 residual. b) The CSC1-CSC2 residual. The curves are the fit by Gaussian plus constant.

In principle two approaches are possible to make up the amplitude finding algorithm. In one of them the maximum position is found at first and then some algorithm is applied in area around maximum to get the value of amplitude. This area may contains several samples. One of the example of such algorithm may be the sum of maximal sample and its nearest neighbours. In order this algorithm works properly the gate should contains at least one sample more from each side then used by algorithm itself. This is needed because the arriving time to fluctuate and narrow

gate may be reason losses some samples. In the second algorithm all samples included in the gate are used no matter how signal places inside it.

Both amplitude finding algorithms were checked. In the both cases the signal was fitted by bipolar function. The bipolar function has four parameters. Two parameters (n and τ) were found by fitting the average signal shape and was then fixed. Another two (T_0 and the amplitude) were determined from the fit of individual signals. The example of the average and the individual signals for five samples gate are shown in fig.5. As result of this study no significant advantage of first algorithm in the chamber position resolution and efficiency was found and second algorithm was chosen for further analysis.

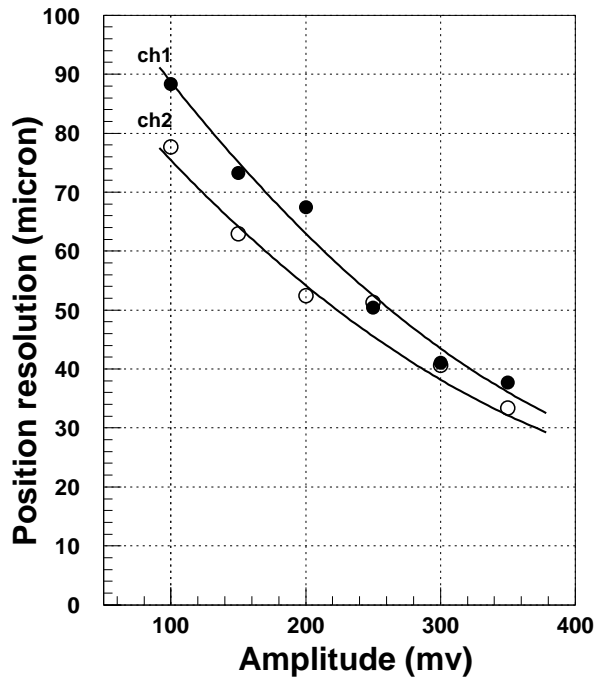


Figure 7: The dependence of the CSC position resolution on the amplitude . The solid and open points are CSC1 and CSC2 layers respectively.

After the amplitude was determined, the procedure of finding the cluster position was applied. For this aim the maximal strip and its nearest neighbours from each side were selected and the cluster position was calculated by the ratio algorithm [3]. The fig.6a,b shows Si-CSC1 and CSC1-CSC2

residuals. Unfortunately, during this beamtest Si telescope resolution contributed to the residual significantly due to the multiple scattering of muons and large distance between Si and CSC. However we have three separate distribution (Si-CSC1, Si-CSC2 and CSC1-CSC2) and therefore are able to define all three values of position resolution. The resolution of Si telescope after extrapolation of the track to CSC position is equal 51 micron. The resolution CSC1 and CSC2 at low rate is 57 and 45 micron respectively.

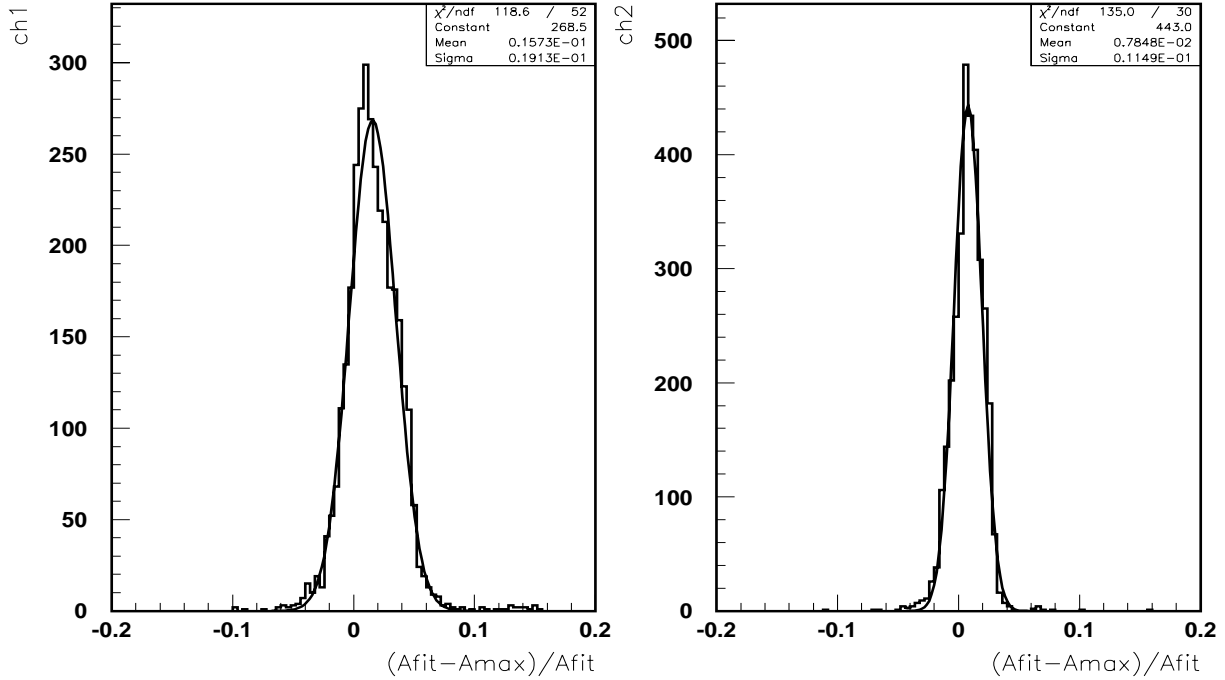


Figure 8: The relative difference of amplitudes found by fitting of signal (A_{fit}) and maximal sample (A_{max}). (a) CSC1 and b) CSC2)

The reason of the position resolution difference of two CSC layers is mainly because of the gas gain in layer CSC2 was 1.5 time higher. If the resolution is compared at the same selected amplitudes the result in the both layers is, practically, the same (see fig.7). The remaining difference can be explained by the fact that the amplitude finding algorithm is less precise for narrower CSC1 signals. This clearly can be seen in fig.8 where the relative difference in amplitudes found from the fit and the maximal sample is shown for both layers. From this figure this difference for the CSC2

layer is significantly less (0.018 for CSC1 and 0.011 for CSC2).

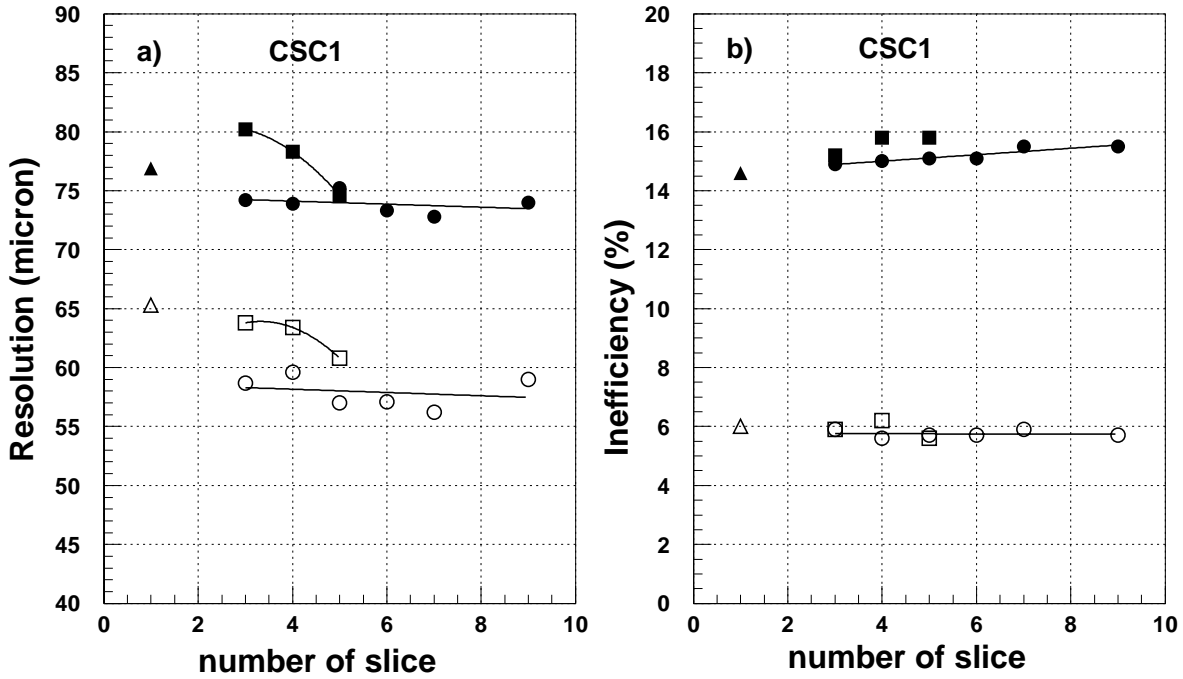


Figure 9: a) The CSC1 position resolution for different amplitude finding algorithms and write clock frequency. The open and solid points are measured at low and high rates respectively. The triangles and circles present the maximal sample and fitting amplitude finding algorithms respectively at standard 40 MHz clock, the squares are the fitting algorithm at 20MHz clock. b) The CSC inefficiency for different amplitude finding algorithms and different clock frequency at high and low background rates.

The fig.9 shows the dependence of the CSC1 position resolution and inefficiency on the number of samples involved in the amplitude finding algorithm. The triangles are the algorithm when the maximal sample is used as amplitude of signal. The circles present the fitting algorithms at different gates. The open and solid points present the measurement at low and high rates respectively. The CSC efficiency is defined as a fraction of events inside the fixed range of $\pm 0.3mm$ the Si-CSC residual (fig.6a). The total number of muons passed through the studied CSC chamber is defined by the Si telescope and another CSC layer. From fig.9b it can be seen that the maximal sample

algorithm gives slightly better efficiency at high rate, however its position resolution is poorer.

The same test beam data was used to check the possibility to apply write clock frequency 20 MHz. The decreasing of clock frequency give the opportunity to increase the depth of SCA pipe line. To simulate 20 MHz clock the amplitude finding algorithm was applied to even (or odd) samples. The final results contain the mixture of events with even and odd samples and are shown in the fig.9 by squares.

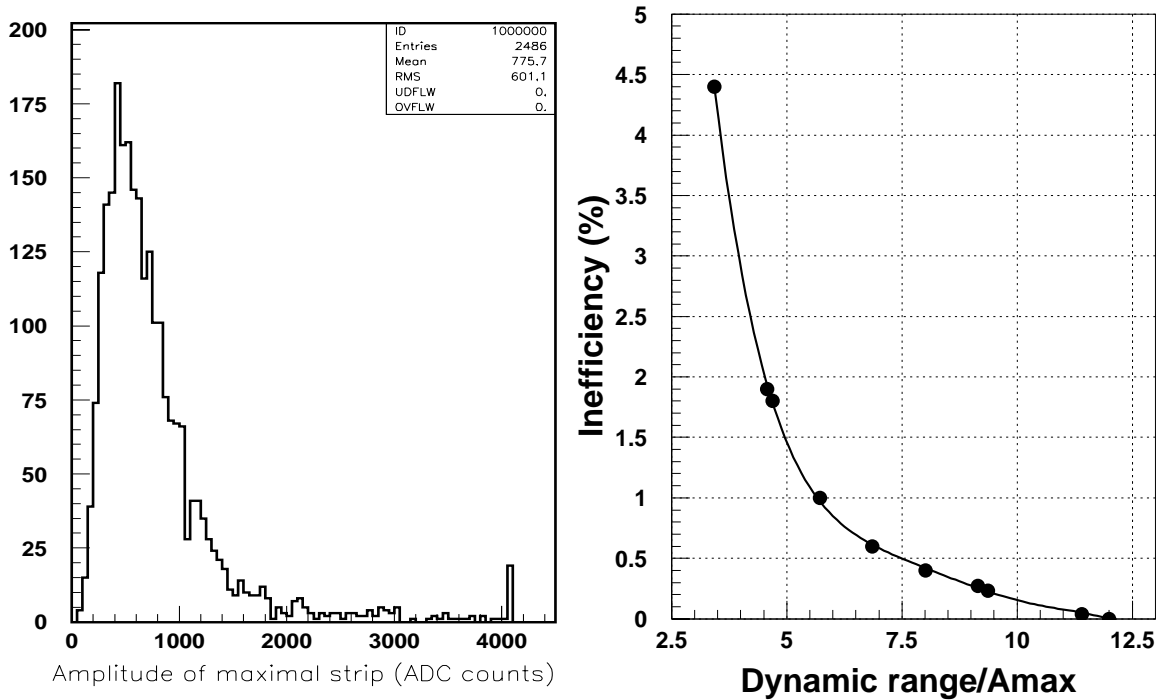


Figure 10: a) The amplitude of maximal strip distribution. The dynamic range of given plot is defined by 12 bits, the signals higher amplitude are accumulated in the end of range. b) the inefficiency versus the value of dynamic range. The range is normalised to the most probable amplitude deposited by muon in the maximal strip.

The next question is how the dynamic range of readout electronics affects on the CSC efficiency. The distribution of amplitude of maximal strip is shown in fig.10a. In the given plot the dynamic range after pedestal subtraction was limited by 12 bits (4096 ADC counts) and amplitudes more than 12 bit accumulated in 4100 channel. It can be seen that the amplitude of signals has the wide

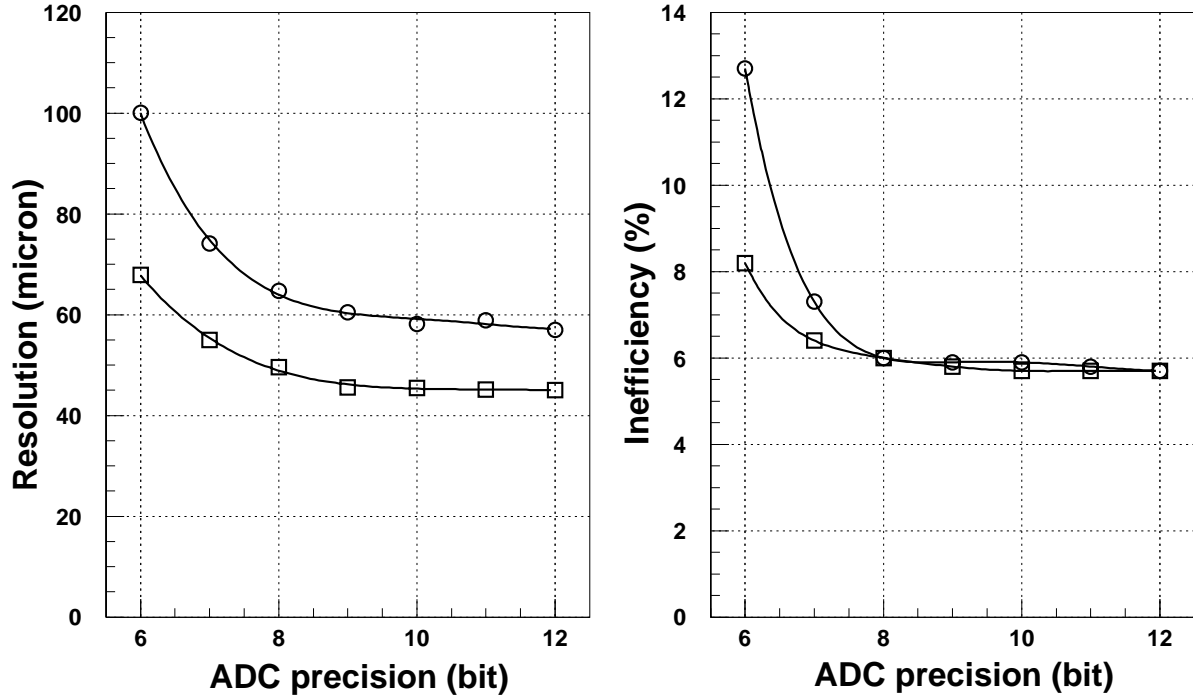


Figure 11: The CSC single plane a) position resolution and b) inefficiency versus the ADC precision. The solid and open points are data for low and high rate respectively. The circles and square points are CSC1 and CSC2 data respectively.

distribution with a long tail and, practically, for any dynamic range the part of signals lays behind the range. Thus the limitation of range decreases the CSC efficiency. The fig.10b shows how CSC efficiency depends on the value of dynamic range. The dynamic range is normalised to the most probable amplitude deposited by the muon in the maximal strip.

The digitization of the amplitude also may be the source of degradation CSC performance. In order to check how the ADC precision affects on the CSC resolution and efficiency we intentionally varied number of K ADC bits when the amplitude was digitized. In this study the normalised dynamic range was fixed for all ADC precision at the values 9.3 and 6.2 for CSC1 and CSC2 respectively (4096 counts at 12 bit ADC precision). The fig.11 shows the dependences CSC resolution (fig.11a) and inefficiency (fig.11b) on the ADC precision. The open and solid points present low and high background rates respectively. The circles and square points present CSC1 and CSC2 layers.

In this study five samples fitting algorithm was used to find amplitude and the ratio algorithm [3] to find the track position. It can be seen from fig.11 that the 10 bits ADC precision is enough in order the digitisation contribution was negligible for both CSC resolution and efficiency.

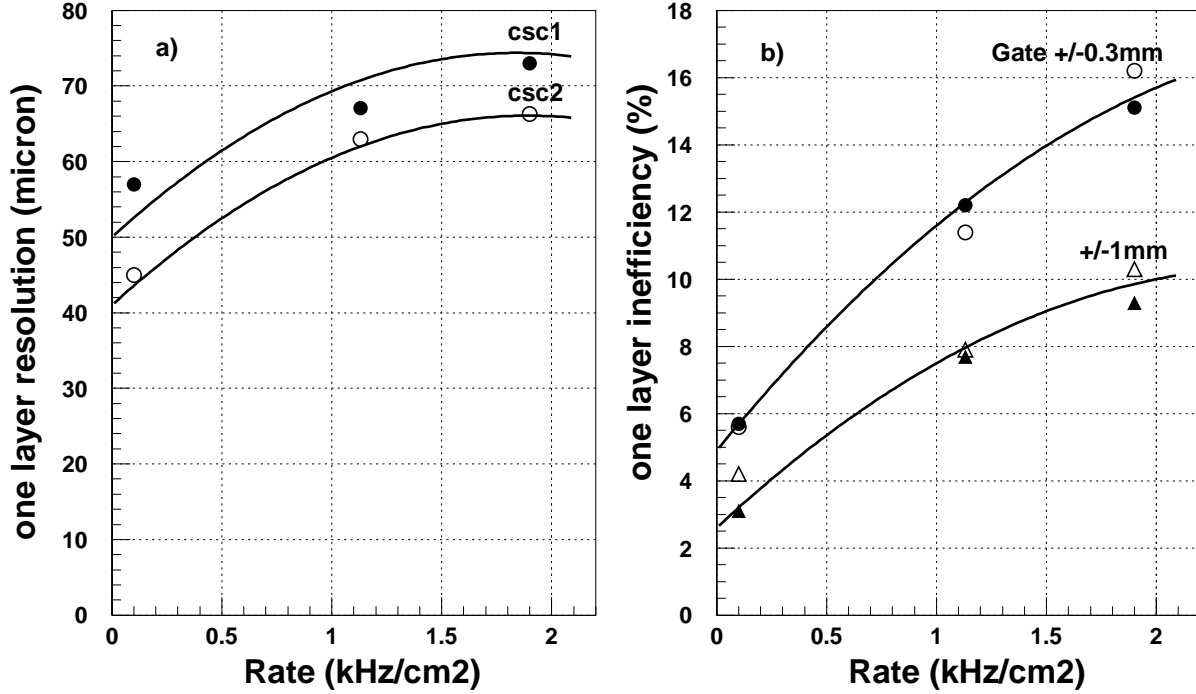


Figure 12: The CSC single plane a) position resolution and b) inefficiency versus the background rate. The solid and open points are data for CSC1 and CSC2 respectively.

The dependence the CSC position resolution (a) and inefficiency (b) on the background rate is shown in fig.12. To determine the amplitude of signal the fitting algorithm and five samples gate samples was applied. The solid and open points are data for CSC1 and CSC2 respectively.

3 Conclusion

During the beamtest the new front-end electronics showed the expected performance. The SCA time scanning readout requires new approach to get the signal amplitude. The CSC performance was checked for several amplitude finding algorithms. As the result it was shown that the four time

samples are enough to save parameters of signal for further analysis without any significant loss information. Also it was shown that the reducing of SCA write clock frequency twice (from 40 to 20 MHz) still does not degrade CSC performance significantly.

Also the dependence of the CSC performance on the ADC precision was studied and it has been shown that ADC precision should be not less than 9 bits in order to neglect this factor. The comparison the results of the previous beamtest analysis showed that at the same condition the results are very similar both for the CSC position resolution and for the CSC efficiency.

4 References

1. G.Bencze et al., Nucl.Instr. and Meth. A 357(1995) 40.
2. V.Gratchev et al., Nucl.Instr. and Meth. A 365(1995) 576.
3. A.Gordeev et al., Atlas note ATL-MUON-2000-005 (ATL-COM-MUON-99-032)